Biosensors and Bioelectronics 126 (2019) 640–646

Contents lists available at ScienceDirect

Biosensors and Bioelectronics

journal homepage: www.elsevier.com/locate/bios

A label-free impedimetric aptasensor for the detection of *Bacillus anthracis* spore simulant

Vincenzo Mazzaracchio[a,1], Daniela Neagu[a,1], Alessandro Porchetta[a], Eleonora Marcoccio[a], Alice Pomponi[b], Giovanni Faggioni[b], Nino D'Amore[b], Andrea Notargiacomo[c], Marial Lilia Pea[c], Danila Moscone[a], Giuseppe Palleschi[a], Florigio Lista[b], Fabiana Arduini[a,*]

[a] Department of Chemical Science and Technologies, University of Rome Tor Vergata, Via della Ricerca Scientifica, 00133 Rome, Italy
[b] Scientific Department, Army Medical Center, Via S. Stefano Rotondo, 00184, Rome, Italy
[c] Institute for Photonics and Nanotechnology-CNR, 00156 Rome, Italy

ARTICLE INFO

Keywords:
Biological warfare agents
Screen-printed electrodes
In situ analysis
Aptamer
Electrochemical impedance spectroscopy

ABSTRACT

Herein, we report an impedimetric DNA-based aptamer sensor for a single-step detection of *B. anthracis* spore simulant (*B. cereus* spore). Specifically, we designed a miniaturized label-free aptasensor for *B. cereus* spores based on a gold screen-printed electrode functionalized with *B. cereus* spores-binding aptamer (BAS-6R). Several parameters were optimized to fabricate the aptasensor such as the concentration of DNA aptamer solution (0.5 μM), the time (48 h), the temperature (4 °C), and the pH (7.5) for aptamer immobilization on the working electrode surface. Once the aptasensor was developed, it was tested against *B. cereus* spores 14579 evaluating the effect of incubation time and $MgCl_2$ concentration. Under the optimized conditions (incubation time equal to 3 h and absence of $MgCl_2$), *B. cereus* spores 14579 were detected with a linear range between 10^4 CFU/ml and 5×10^6 CFU/ml and a detection limit of 3×10^3 CFU/ml. Furthermore, the study of selectivity toward *B. cereus* 11778, *B. subtilis*, *Legionella pneumophila*, and *Salmonella* Typhimurium has demonstrated the capability of this sensor to detect *B. cereus* spores, proving the suitability of the DNA-based sensing element combined with a portable instrument for a label-free measurement on site of *B. anthracis* spore simulant.

1. Introduction

In 1972 Organization for the Prohibition of Chemical Weapons (OPCW) organized a convention on the prohibition of the development, production, and stockpiling of bacteriological (biological) and toxin weapons, establishing fifteen articles for biological and toxin weapon management. However, these warfare agents were used in the last centuries as weapons for mass destruction and terrorist attacks (Atlas, 2002; Barras and Greub, 2014), exploiting their high toxicity combined with easiness of production and with the difficulty for their early detection (Thavaselvam and Vijayaraghavan, 2010). Among several biological warfare agents, *Bacillus anthracis (B. anthracis)* has been at the forefront of political and scientific debate in 2001, because it was used by terrorists to contaminate letters of USA citizens, resulting in five deaths.

B. anthracis is a Gram-positive spore-forming bacteria belonging to the *Bacillus cereus* group (Turnbull, 1999), is the etiological agent of anthrax, a zoonosis which affects mainly herbivores. The natural spread of the disease occurs through the contact with the spores (the infectious form of *B. anthracis*), generally released into the soil following the dead of the host (Mock and Fouet, 2001). Even if uncommon, anthrax is one of the human occupational diseases, since humans may acquire the infection directly by contact with infected livestock, or indirectly by handling contaminated products. Three major routes of human infection are recognized: i) through the skin (cutaneous anthrax), ii) by ingestion (gastrointestinal anthrax), or iii) by inhalation (pulmonary anthrax) (Plotkin and Grabenstein, 2008). Cutaneous anthrax, which is the most common form, has the lowest mortality rate (< 1%) since it is easy to recognize and can be quickly treated with antibiotics. Conversely, both gastrointestinal and pulmonary anthrax are difficult to detect in the early phase of infection, resulting in systemic septicemia leading often to an irreversible injury. The mortality rate of pulmonary anthrax is higher than 80%. These features along with the relatively simple production of the spores as well as the possible biomolecular engineering (i.e. drug resistance), make *B. anthracis* one of the most eligible biological weapons (Goel, 2015).

* Corresponding author.
E-mail address: fabiana.arduini@uniroma2.it (F. Arduini).
[1] These authors contributed equally.

https://doi.org/10.1016/j.bios.2018.11.017
Received 23 September 2018; Received in revised form 12 November 2018; Accepted 13 November 2018
Available online 15 November 2018
0956-5663/

For a prompt and effective management of terroristic attacks via *B. anthracis* spores, fast and miniaturized analytical tools integrated within portable devices could be very useful for fast tackling of the event with properly countermeasures.

Unfortunately, routine methods for *B. anthracis* spore detection rely on bacteriological characterization or rapid viability PCR method (Dixon et al., 1999; Qi et al., 2001; Hurtle et al., 2004; Dang et al., 2001). In the first case, the measurement requires several days for the evaluation of colony color, morphology of the bacteria, motility lack, gamma fagi diagnosis, and hemolytic activity lack. In the second case, the use of the polymerase chain reaction has the advantages to identify spores from swab or air sample with a short time analysis and a low detection limit. For instance, Makino et al. (2001) reported a detection of one spore in 100 l of air sample while Higgins et al. (2003) were able to detect 3700 spores in one m^3. However, these methods require a laboratory set up, expensive instrumentation, and skilled personnel.

Alternative methods are based on immunological assays, exploiting the interaction between the labeled antibody and the antigen over exosporium, like BclA (Swiecki et al., 2006), reaching detection limits at the level of 10^3 spore/ml (Tamborrini et al., 2010). For the immunoassay development, the production of antibodies requires the use of animals, and a further drawback is that the antibodies are often characterized by short lifetime in working and storage condition. In order to overcome these drawbacks, synthetic short single stranded nucleic acid sequences, namely aptamers, represent a forefront technology for biosensing applications, because of their unique properties in terms of stability and specificity for the target analyte (Ellington and Szostak, 1990; Tuerk and Gold, 1990; Jayasena, 1999; Mairal et al., 2008; Song et al., 2008). Thanks to these fascinating properties, aptamers have been widely used as recognition elements for biosensor development, and they are generally modified with optical or electrochemical labels to achieve real-time transduction of the binding event between the DNA probe and the target analyte. Optical aptasensors were applied for the detection of several targets, including thrombin (Bini et al., 2007), ochratoxin (Yang et al., 2011), glycated haemoglobin (Eissa and Zourob, 2017), and cocaine (He et al., 2010; Porchetta et al., 2012). Most of them exploit structure-switching mechanisms to transduce the target binding into a readable optical output. Alternatively, the use of electrochemical impedance spectroscopy does not require any label by delivering a cost-effective label-free aptasensor. This approach thus presents several advantages compared to amperometric and potentiometric biosensors (Labib et al., 2012; Eissa et al., 2013).

Herein, we describe the first miniaturized and label free aptasensor for the detection of *B. anthracis* spores. Specifically, we explored the possibility of using *B. anthracis* spores-binding DNA aptamer (BAS-6R), developed for fluorescence analysis (Bruno and Carrillo, 2012), in an electrochemical fashion by simply immobilizing the aptamer on a gold-based printed electrode. To immobilize BAS-6R aptamer on the gold surface of a screen-printed electrode (SPE), it was modified with a thiol group at 5′ end, exploiting the high affinity of thiol for the gold surface. To evaluate the binding between the aptamer and the spore, the resistance to charge transfer (R_{ct}) of the ferro/ferricyanide redox probe was evaluated by means of electrochemical impedance spectroscopy technique. To follow a biosafety protocol, we have used *B. cereus* spores as simulant, in agreement with the simulant used by Bruno and Carrillo (2012).

2. Experimental section

2.1. Materials

Bacillus cereus ATCC 11778, *Bacillus cereus* ATCC 14579, and *Bacillus subtilis* ATCC 6633 strains were purchased from Oxoid-Thermofisher and spores were produced by Scientific Department of Army Medical Center (Italy). Reagents of analytical grade were used without further purification. The aptamer BAS 6R (5′ATCCGTCACACCTGCTCTGCACG GGCTCAGTTTGGCTTTGTATCCTAAGAGGATGGT

GTTGGCTCCCGTAT-3′) was selected accordingly Bruno and Carrillo (2012) and purchased from Sigma-Aldrich with thiol modification at 5′ end. The aptamer was stored in Tris-HCl Buffer 100 mM + $MgCl_2$ 1 mM (25 μM stock solution) at −20 °C until use. The spores were stored at −18 °C in phosphate buffer solution. *Salmonella* Typhimurium and *Legionella pneumophila* WDCM 00107 was purchased from Oxoid and Sigma-Aldrich, respectively. For safety condition, *Salmonella* Typhimurium was boiled while *Legionella* was treated 20 min at 95 °C.

2.2. Screen-printed electrode fabrication

Gold-based screen-printed electrodes (Au-SPEs) were home-produced with a 245 DEK (Weymouth, UK) machine. The working electrode was printed using gold-ink BQ331, Dupont, while the pseudo-reference electrode was printed using silver-based ink (Electrodag 477 SS) and the counter-electrode using graphite-based ink (Electrodag 421), both from Acheson (Milan, Italy). Electrodes were printed on a flexible polyester substrate (Autostat HT5) from Autotype Italia (Milan, Italy), with thickness of 0.175 mm. An insulator (Argon Carbonflex 25.101S) was used to define the working surface area, which resulted in a diameter of 3 mm. The printing procedure used has been already described in our previous papers (Arduini et al., 2012, 2015).

2.3. Instrumentation

Both cyclic voltammetric (CV) and Electrochemical Impedance Spectroscopy (EIS) experiments were carried out with a portable potentiostat PalmSens^3 (PalmSens Instrument), connected to a laptop equipped with PsTrace software. Atomic force microscopy (AFM) characterization of the aptasensor in presence and in absence of the spores was performed by using a Veeco-Digital Instruments D3100 microscope with a Nanoscope IIIa controller operated in air environment. Tapping Mode probes with nominal tip curvature radius of 5 ÷ 10 nm and spring constant ~40 N/m were employed.

2.4. Pre-treatment of Au-SPEs

To obtain a gold working electrode surface characterized by a satisfactory repeatability, each electrode was dipped in the piranha solution (H_2SO_4/H_2O_2 3:1 (v/v)) until the gold surface became black, followed by a rinse step with distilled water. Successively, the working electrode surface was electrochemically treated by using 20 scans of cyclic voltammetry in the range between −0.4 V and 1.5 V, with a scan rate of 100 mV/s, using H_2SO_4 0.1 M as electrolyte.

2.5. Pre-treatment of the aptamer

To obtain a high stable aptamer conformation on the gold surface, the procedure reported by Zhou et al. (2012) was used with some modifications. Briefly, the aptamer was denatured by heating the aptamer solution at 95 °C for 5 min; then it was cooled at 4 °C for 15 min. A final step, consisting in maintaining the solution at 25 °C for 5 min was required to renaturate the aptamer.

2.6. Preparation of aptasensor

To immobilize the aptamer on the gold working electrode surface, 20 μl of the aptamer solution at the concentration of 0.5 μM in Tris HCl Buffer 100 mM + $MgCl_2$ 1 mM were deposited over the gold working electrode surface. Afterwards, Au-SPEs were incubated at 4 °C for two days. Subsequently, the aptamer-modified Au-SPEs were washed with distilled water, followed by a blocking step with 20 μl of 6-mercaptohexanol in Dulbecco buffer solution left for 2 h on the gold working electrode surface.

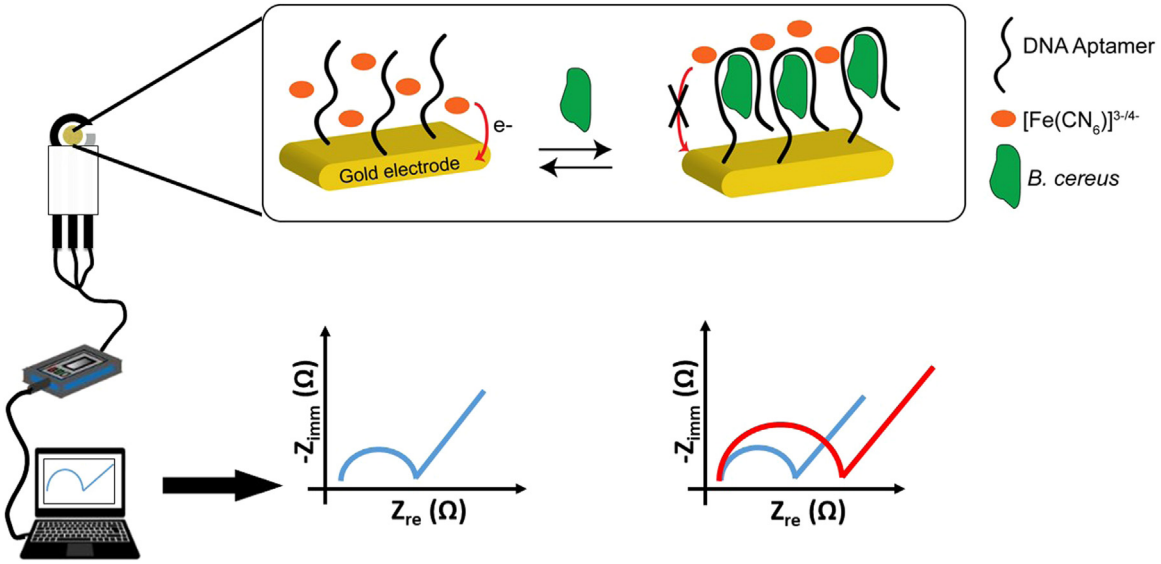

Fig. 1. Scheme of principle for *B. anthracis* spore (*B. cereus)* simulant detection and experimental set-up for EIS measurement using miniaturized aptasensor.

2.7. B. cereus spore measurement

The detection of *B. cereus* spore, after the immobilization of the aptamer on the Au-SPE, was carried out by EIS measurements (Fig. 1). The EIS measurements were performed setting the following parameters: fixed potential, Edc: 0.0 V, Eac: 0.01 V, Number of frequencies: 41, max. frequency: 10,000 Hz, min. frequency: 1 Hz, min. sampling time: 0.5 s, max. equilibrium time: 1 s, OCP max. time: 1 s, stability criterion: 0.001 mV/s.

The detection of *B. cereus* spore was carried out accordingly to the following protocol: the aptasensor was incubated at 37 °C for three hours with 20 µl of *B. cereus* spore solution in phosphate buffer. Later, the aptasensor was rinsed with phosphate buffer and the aptasensor was immersed in 10 ml of KCl 0.1 M solution containing 2.5 mM $[Fe(CN)_6]^{3-/4-}$ to carry out the EIS measurements. The resistance to charge transfer was calculated using Randles circuit and Z-View software.

2.8. B. cereus spore measurement in air

The air sampling was performed using SASS 4000 portable aerosol pre-concentrator (4000 L/min) combined with a portable air sampler (SASS 2300) to obtain an aqueous sample to analyse. The sampling was performed outdoor on October 25th, 2018 (latitude: N 41.88573535°, longitude: 12.50098557°) for consecutively 24 h. At the end of this sampling procedure, 8 ml of water was collected and immediately frozen at −20 °C. For the analysis, the sample of water was diluted 1:10 v/v in working buffer and analysed as described in Section 2.7

3. Results and discussion

The principle of this sensor relies on the binding of the spore with the immobilized aptamer, producing an aptamer-spore interaction on the working electrode surface that hinders the electron-transfer of $Fe(CN)_6^{3-}/Fe(CN)_6^{4-}$, thus producing an increase of R_{ct} values, proportional to the amount of spores.

To achieve a good repeatability, firstly we investigated the treatment of the working electrode surface and of the aptamer. After that, the different working conditions for aptamer immobilization as well as for the binding between aptamer and *B. cereus* spores were investigated to deliver an aptasensor with satisfactory analytical performances in terms of repeatability and sensitivity. Finally, a morphological characterization of the aptasensor was performed to confirm the binding between the surface-confined aptamer and *B. cereus* spores not before investigated.

3.1. Modification of the SPE surface with the DNA aptamer

To develop a sensitive and repeatable aptasensor, the surface of the Au-SPEs was firstly pre-treated with a specific protocol to enhance the electrochemical performances, allowing the formation of a compact self-assembled monolayer. Many studies have been reported in literature on the use of different approaches for electrode surface treatment (Hamelin, 1996; Carvalhal et al., 2005; Xiao et al., 2007). Often, a gold electrode requires the treatment of the working surface using, for instance, cyclic voltammetry as technique and H_2SO_4 as working solution. Herein, we pre-treated the gold electrode surface exploiting the piranha solution for few seconds, followed by electrochemical treatment using cyclic voltammetry and H_2SO_4 (Pagliarini et al., 2018). The effect of this treatment on the repeatability of aptasensor was evaluated by immobilising the aptamer on untreated and treated Au-SPE and evaluating R_{ct} value in EIS using $[Fe(CN)_6]^{3-/4-}$ as electrochemical probe. As reported in Fig. 2A, this treatment results in a sensor characterized by improved electrochemical performances, and in a decrease of resistance to charge transfer value mean from 270 to 160 Ω, for treated Au-SPEs. Furthermore, using the treated Au-SPE, an improvement of the repeatability of the sensor was achieved, with a RSD % decrease from 25 to 10 in the case of un-treated and treated Au-SPE (n = 10), respectively. For this reason, the treated Au-SPE was used as platform to immobilize the DNA aptamer. The DNA aptamer has been previously treated at 95 °C for 5 min followed by a quickly cooled at 4 °C for 15 min. Successively, a further step at room temperature was used to allow the aptamer folding which is an essential condition to bind *B. cereus* spores. The advantage of using this treatment has been already reported for many aptamers with a high number of nucleotides (Zhou et al., 2012). As reported in Fig. 2B, also this treatment confers to the system a better repeatability with a RSD % equal to 10, which is an improved value in comparison with what obtained for the immobilization of the un-treated aptamer (RSD % = 65). Thus, this treatment was employed before the aptamer immobilization.

3.2. Investigation of experimental conditions effect on the DNA-based self-assembly monolayer

To allow an effective and reliable impedimetric aptasensor, the fine control of the morphology of the electrode and the optimization of the experimental conditions to achieve reproducible self-assembled

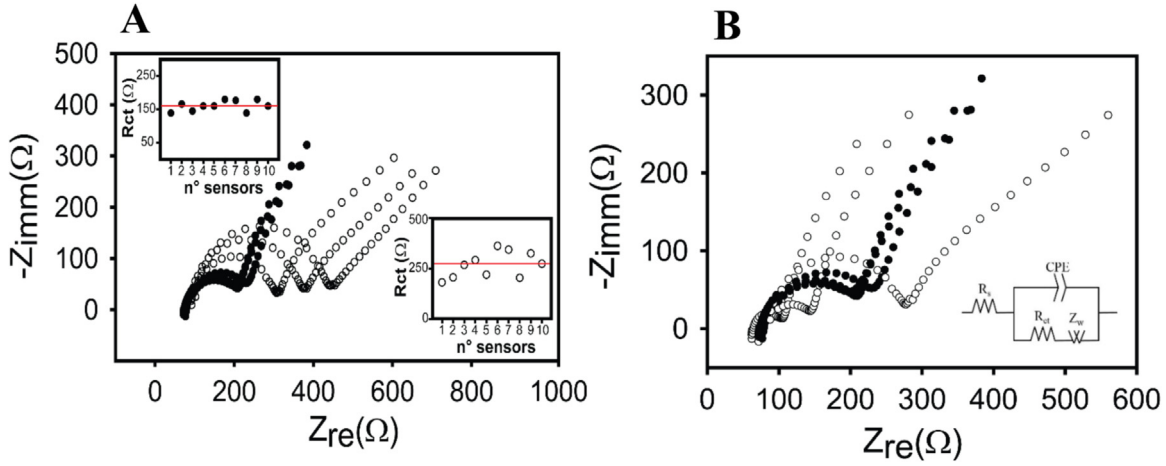

Fig. 2. (A) Nyquist plot of EIS measurement of SPEs modified with the temperature-treated aptamer with (black circle) and without piranha pre-treatment (white circle) (n = 3). Measurements performed in $[Fe(CN)_6]^{3-/4-}$ 2.5 mM + KCl 0.1 M, after incubation of SPE at 4 °C for 18 h with aptamer 0.5 μM. Inset: The repeatability of the aptasensor using ten different SPEs with (black circle) and without piranha pre-treatment (white circle). (B) Nyquist plot of EIS measurements of SPEs modified with temperature-treated aptamer (black circle) and without temperature-treated aptamer (white circle). Measurements performed in $[Fe(CN)_6]^{3-/4-}$ 2.5 mM + KCl 0.1 M, after incubation of the SPEs at 4 °C, for 18 h with aptamer concentration of 0.5 μM, pH 7.5. Inset: Randles circuit used to fit the data which includes electrolyte solution resistance, R_S, the charge transfer resistance, R_{ct}, in series with the Warburg impedance, Z_W, and in parallel with a constant phase element, CPE.

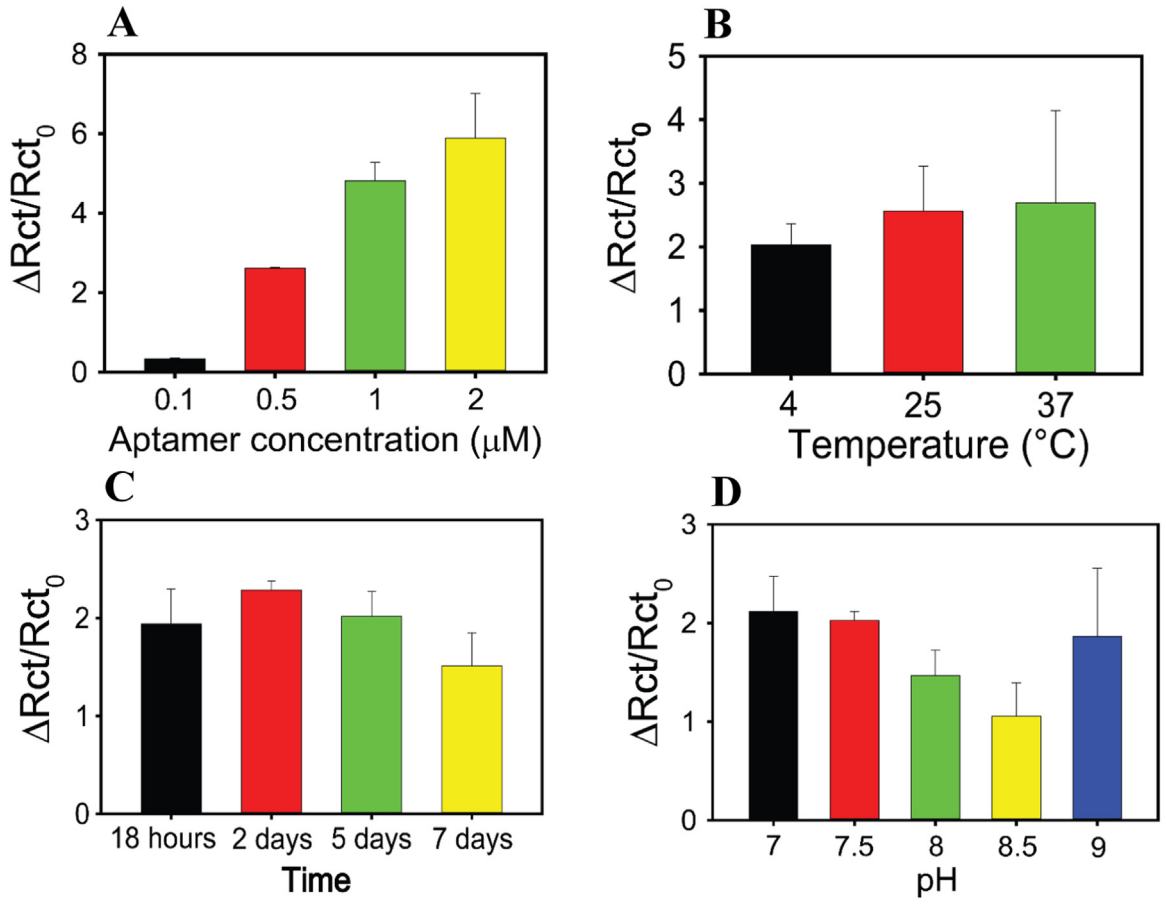

Fig. 3. (A) Histogram bars of ΔR_{ct} / R_{ct0} using four different aptamer concentrations, namely 0.1 μM, 0.5 μM, 1 μM and 2 μM. (B) Histogram bars of ΔR_{ct} / R_{ct0} for aptamer incubation at 4 °C (black), 25 °C (red) and 37 °C (green), for 18 h in TRIS-HCl 0.1 M + $MgCl_2$ 1 mM, pH 7.5. (C) Histogram bars of ΔR_{ct} / R_{ct0} using incubation time of 18 h (black), 2 days (red), 5 days (green) and 7 days (yellow), in TRIS-HCl 0.1 M + $MgCl_2$ 1 mM, pH 7.5. (D) Histogram bars of ΔR_{ct} / R_{ct0} using buffer TRIS-HCl 0.1 M + $MgCl_2$ 1 mM, pH 7 (black), 7.5 (red), 8 (green), 8.5 (yellow) and 9 (blue), immobilization at 4 °C for 2 days. Measurements were performed in 2.5 mM $[Fe(CN)_6]^{3-/4-}$ + KCl 0.1 M, using an aptamer concentration of 0.5 μM. (For interpretation of the references to color in this figure legend, the reader is referred to the web version of this article.)

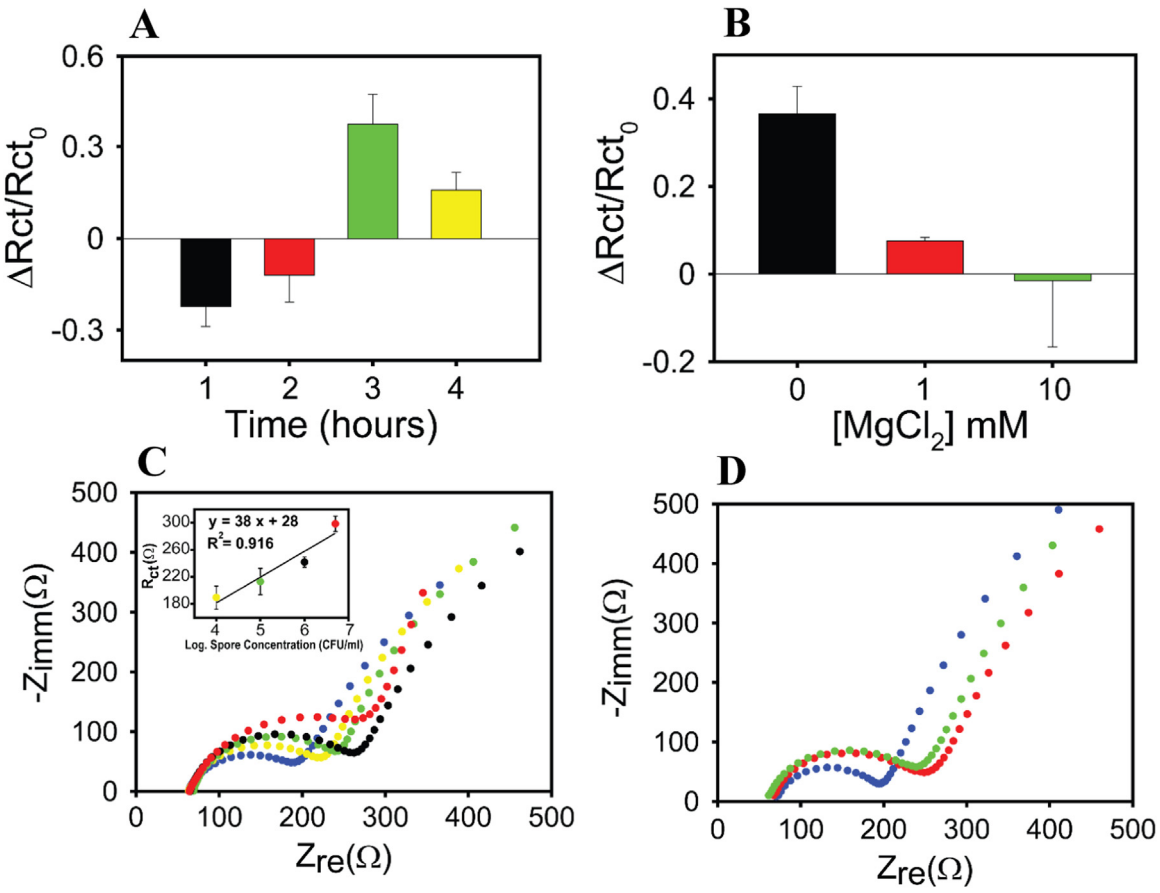

Fig. 4. : (A) Study of incubation time using 1 h (black), 2 h (red), 3 h (green), 4 h (yellow), at 37 °C using *B. cereus* 14579 spores at concentration equal to 10^5 CFU/ml. (B) Study of $MgCl_2$ concentration effect: 0 (black), 1 mM (red), 10 mM (green), incubation at 37 °C for 3 h, using *B. cereus* 14579 spores at concentration equal to 10^5 CFU/ml. (C) Nyquist plot obtained using different concentrations of *B. cereus* 14579 spores: blank (blue), 10^4 CFU/ml (yellow), 10^5 CFU/ml (green), 10^6 CFU/ml (black), 5×10^6 CFU/ml (red). Inset: Calibration curve of the logarithm of the spore concentration vs the R_{ct} value. (D) Nyquist plot obtained when the air sample, collected and diluted 1:10 v/v with working buffer, was analysed with (green line) and without (blue line) the addition of 5×10^6 CFU/ml. For a comparison, Nyquist plot of 5×10^5 CFU/ml in standard solutions was reported in a red line. (For interpretation of the references to color in this figure legend, the reader is referred to the web version of this article.)

monolayers are crucial. To this regard, we evaluated the variation of R_{ct} values varying several working conditions, namely the concentration of the aptamer in solution that results in different surface densities on the gold electrode surface, the temperature, time of incubation, and the pH of the buffer solution. In order to minimize the variability, the relative variation of R_{ct} ($\Delta R_{ct}/R_{ct0}$) was used (Sheikhzadeh et al., 2016). This value was calculated as follows:

$$\Delta R_{ct}/R_{ct0} = (R_{ct\ after} - R_{ct0})/R_{ct0}.$$

where $R_{ct\ after}$ and R_{ct0} represent the electrochemical signals in the presence and in the absence of DNA aptamer on the gold surface.

To identify the optimal concentration of the DNA aptamer, four different concentrations were tested, namely 0.1 μM, 0.5 μM, 1 μM, and 2 μM (Fig. 3A). As shed light in Fig. 3A, by increasing the aptamer concentration in solution, we observed an increase of the variation of R_{ct}, due to the higher surface density of the DNA aptamer on the gold-pretreated working electrode surface (Ricci and Plaxco, 2008). In detail, we have observed $\Delta R_{ct}/R_{ct0,}$ values equal to 2.61, 4.82 and 5.89 for aptamer concentration of 0.5 μM, 1 μM, and 2 μM, respectively. Taking into account the repeatability values, 0.5 μM (RSD % = 1%), against 1 μM (RSD % = 10%), and 2 μM (RSD % = 19%), 0.5 μM value was chosen for the further studies.

The effect of temperature of the SAM was then evaluated by testing the aptasensor response in absence of the spore, when immobilised at 4 °C, 25 °C, and 37 °C. Fig. 3B shows that by increasing the temperature, the repeatability decreases, probably due to the effect of temperature on the aptamer structure, thus a temperature of 4 °C was selected for aptamer immobilization.

Furthermore, the incubation time of the DNA aptamer on the gold electrode to generate the SAM was also investigated. Specifically, the response of the aptasensor after an incubation time of 18 h, 2 days, 5 days, 7 days at 4 °C was evaluated. As depicted in Fig. 3C, the highest repeatability of $\Delta R_{ct}/R_{ct0}$ signal was obtained with 2 days of incubation of the aptamer on the electrode, thus this value was selected for the further studies.

Finally, we also tested different pHs of the same incubation buffer ranging from 7 to 9, in order to evaluate the pH effect on the formation of the SAM. As expected, the optimal pH resulted 7.5 as shown in Fig. 3D.

3.3. Optimization of the experimental condition for B. cereus spore detection

Once optimized the conditions to immobilize the aptamer, we investigated the effect of different experimental conditions like the incubation time and $MgCl_2$ concentration to achieve the highest affinity binding with spores (*B. cereus*, here employed at the fixed concentration of 10^5 CFU/ml). First, we evaluated how the different incubation times can affect the binding between the spores and the immobilized aptamer. As showed in Fig. 4A four different times were tested (i.e. 1 h, 2 h, 3 h and 4 h), revealing negative $\Delta R_{ct}/R_{ct0}$ signal for less than 3 h of incubation and positive with 3 h and 4 h of incubation. In the first case,

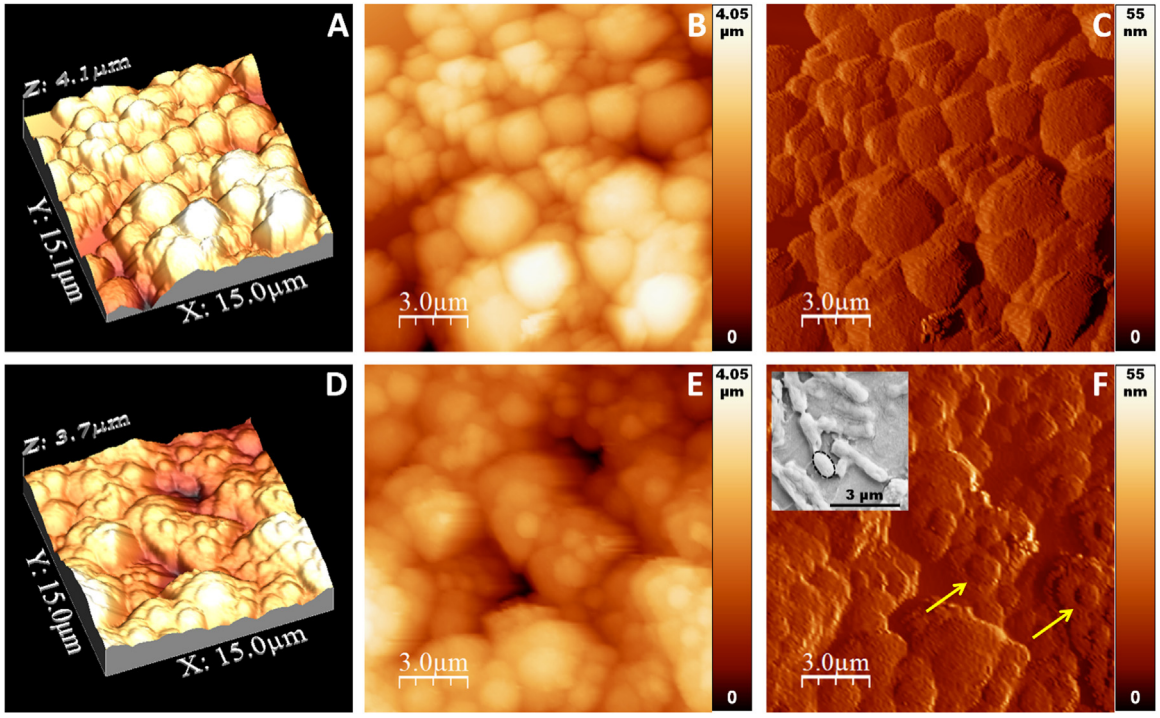

Fig. 5. AFM images of the gold working electrode surface functionalized with the aptamer BAS-6R: (A) 3D and (B) 2D views, and (C) Tapping Mode amplitude signal. AFM images after exposing the aptamer functionalized gold working electrode to a solution containing spores: (D) 3D and (E) 2D views, and (F) Tapping Mode amplitude signal. Arrows in panel F highlight two of the rounded structures covering quite uniformly the aptamer functionalized gold surface; the inset shows the SEM micrograph of *Bacillus cereus* spores deposited on the aluminium substrate with a dashed contour highlighting a spore.

the time was not sufficient for an optimal spore-aptamer interaction and the introduction of the spores into the system probably generates morphological changes, giving a negative $\Delta R_{ct}/R_{ct0}$ value. After 3 h of incubation, an optimal binding between the spores and the aptamer was reached, leading to an increasing of the $\Delta R_{ct}/R_{ct0}$ value. Thus, next measurements were carried out by using 3 h as the time for spore incubation.

After we investigated if $MgCl_2$ could improve the binding of spores to the aptamer, because it is well known (Record, 1975) that the presence of divalent cations (especially Mg^{2+}) can strongly affect the DNA-based receptor and target interaction. As reported in Fig. 4B, we tested two different concentrations of $MgCl_2$ (i.e. 1 mM and 10 mM) and $\Delta R_{ct}/R_{ct0}$ signals reported clearly indicate that the presence of this divalent cation affects the binding with the spore. This can be ascribed to a shielding effect of the divalent cation Mg^{2+} on the DNA aptamer, because divalent cations can stabilize both the DNA aptamer in its native conformation and the aptamer/target complex and these two effects can both affect the overall affinity and sensitivity of the system. Thus the successive binding study was carried out in absence of $MgCl_2$ (Fig. 4B).

3.4. Analytical features of the sensing platform

To investigate the analytical features of this aptasensor, a calibration curve was obtained using different concentrations of *B. cereus* 14579 spores, in the range of concentration between 10^4 CFU/ml and 5×10^6 CFU/ml (Fig. 4C). A linear dependence of R_{ct} on logarithm of the spores concentration was indicated by the following equation $y = 38x + 28$ ($R^2 = 0.918$) with a limit of detection (LOD) equal to 3×10^3 CFU/ml, calculated as $3(S_b/m)$ where S_b is standard deviation of the blank signal and m the slope of the calibration curve.

The selectivity of the aptasensor was evaluated testing other two types of *Bacillus* spore, namely *B. cereus* 11778 and *B. subtilis* and two different bacteria namely *Legionella pneumophila* and *Salmonella* Typhimurium. The response against the two different *B. cereus* spores is comparable, while *B. subtilis* 6633 spores showed a slight low value while any response was observed in the case of *Legionella pneumophila* and *Salmonella* Typhimurium bacteria (data not shown). This behavior is probably ascribed to the differences present in *B. subtilis* and *B. cereus* exosporium, indeed the two *B. cereus* spores have a similar exosporium when compared with the exosporium of *B. subtilis*. The completely different structure of *Legionella pneumophila* and *Salmonella* Typhimurium avoids the binding with aptamer, allowing for the absence of R_{ct} increase.

To confirm the applicability of this sensor in real matrices, the aptasensor was tested measuring an air sample. Since the aptasensor is able to detect the spore in aqueous solution, a combined system constituted of SASS 4000 and SASS 2300 was used, being able to sampling the air, extract particulates and water-soluble chemical vapors from air and transfers them in a liquid phase (water). The aqueous sample was then diluted 1:10 v/v in the working buffer to avoid any matrix effect for the presence of particulate material. As depicted in Fig. 4D, Nyquist plot obtained analyzing the sample is comparable to the one observed using an aptasensor without spore-binding, demonstrating the absence of the spore at the limit of detection. The aptasensor was then tested with the same sample fortified with *B. cereus* spores 14579 (sample spiked with 5×10^6 CFU/ml and diluted 1:10 v/v with working buffer), giving a similar response of 5×10^5 CFU/ml in standard solution with a satisfactory recovery value, i.e. 99 ± 12 (%).

3.5. Morphological characterization

AFM investigation was performed to confirm the binding between the immobilized aptamer and the spores. Fig. 5 (A, B, and C) shows the AFM morphology collected on a gold working electrode surface functionalized with the aptamer. The 2D and 3D views of topographic height data (Fig. 5A and B) show the typical grainy morphology of the working electrode due to the presence of Au particles, which size ranges

between ~1 μm and ~4 μm. The particles display an apparent faceting with large plateaus of few microns, as more clearly evidenced by the Tapping Mode amplitude signal reported in Fig. 5C. Fig. 5 (D, E, and F) shows the AFM investigation of an aptamer working electrode after exposure to a solution of 10^5 CFU/ml of *B. cereus* 14579 spores. A large amount of rounded or slightly elongated structures with size in the range $0.8 \div 1.2$ μm and aspect ratio close to 1 are found to decorate the aptamer functionalized surfaces. Two of these structures are highlighted with arrows in panel F.

The inset of Fig. 5F shows a SEM micrograph of *B. cereus* spores deposited on aluminium substrate. The spores have an elongated structure (aspect ratio > 1.5) with diameter and length in the range of $1 \div 2$ μm, in agreement with data reported in literature (Carrera et al., 2007). For better comparison, the AFM maps and the SEM image are reported using the same length scale. The typical dimensions of the spores are compatible with the structures found in our AFM data, which we therefore identify with the spores. The lower aspect ratio found for the spores in our samples is likely related to the capability of the aptamer to re-arrange its structure along the spores, allowing for a change of the surface morphology in agreement with EIS measurements, however further studies are needed to better investigate the conformation of the aptamer/spore complex onto the gold electrode surface. No clear trace of faceting and plateaus on gold grains are visible in Fig. 5F (compare with Fig. 5C) pointing to a considerable spore coverage.

4. Conclusions

Herein, we reported the first electrochemical aptasensor for the detection of *B. anthracis* spore simulant namely *B. cereus* spores. The aptasensor relies on a gold-screen printed electrode modified with BAS-6R aptamer, exploiting the high affinity of the thiol group present at 5' end of the aptamer with the gold surface of the-screen printed electrode. The measurement of the binding between the immobilized aptamer and the spores was carried out by using the electrochemical impedance spectroscopy, delivering a label free measurement using a portable instrument (PalmSens^3). Several parameters were investigated for the immobilization of the aptamer (i.e. pH, amount of aptamer, temperature, incubation time) as well as for the binding reaction between the immobilized aptamer and the spores (i.e. incubation time and $MgCl_2$ concentration). The aptasensor developed has demonstrated the capability to detect *B. cereus* spores in the range between 10^4 CFU/ml and 5×10^6 CFU/ml with a detection limit of 3×10^3 CFU/ml. The morphological study suggested that the aptamer could be capable to arrange its structure along the spore, allowing for a change of the surface in agreement with electrochemical impedance spectroscopic measurements.

Taking into account the relevant features of this biosensor such as: i) the use of more stable and animal-free DNA instead of other biocomponents e.g. antibody, ii) the requirement of a low amount of the sample (i.e. few μl), iii) the electrochemical technique which allows for a fast measurement using a portable instrument, and iv) the cost-effectiveness, this device can be considered as an useful analytical tool for security monitoring and for the fast management of the terroristic attacks.

Acknowledgements

F.L. and F.A. acknowledge the Italian Ministry of Defence for financial support, Project APTAMERI BW. F.A. acknowledges Prof. Ilaria Cacciotti, University of Rome Niccolò Cusano for SEM analysis.

References

Arduini, F., Di Nardo, F., Amine, A., Micheli, L., Palleschi, G., Moscone, D., 2012. Electroanal 24, 743–751.
Arduini, F., Forchielli, M., Amine, A., Neagu, D., Cacciotti, I., Nanni, F., Moscone, D., Palleschi, G., 2015. Microchim. Acta 182, 643–651.
Atlas, R.M., 2002. Annu. Rev. Microbiol. 56, 167–185.
Barras, V., Greub, G., 2014. Clin. Microbiol. Infec. 20, 497–502.
Bini, A., Minunni, M., Tombelli, S., Centi, S., Mascini, M., 2007. Anal. Chem. 79, 3016–3019.
Bruno, J.G., Carrillo, M.P., 2012. J. Fluoresc. 22, 915–924.
Carrera, M., Zandomeni, R.O., Fitzgibbon, J., Sagripanti, J.L., 2007. J. Appl. Microbiol. 102, 303–312.
Carvalhal, R.F., Sanches Freire, R., Kubota, L.T., 2005. Electroanal 17, 1251–1259.
Dang, J.L., Heroux, K., Kearney, J., Arasteh, A., Gostomski, M., Emanuel, P.A., 2001. Appl. Environ. Microbiol. 67, 3665–3670.
Dixon, T.C., Meselson, M., Guillemin, J., Hanna, P.C., 1999. New Engl. J. Med. 342, 815–826.
Eissa, S., Ng, A., Siaj, M., Tavares, A.C., Zourob, M., 2013. Anal. Chem. 85, 11794–11801.
Eissa, S., Zourob, M., 2017. Sci. Rep. 7, 1016.
Ellington, A.D., Szostak, J.W., 1990. Nature 346, 818–822.
Goel, A.K., 2015. World J. Clin. Cases 3, 20–33.
Hamelin, A., 1996. J. Electroanal. Chem. 407, 1–11.
He, J.L., Wu, Z.S., Zhou, H., Wang, H.Q., Jiang, J.H., Shen, G.L., Yu, R.Q., 2010. Anal. Chem. 82, 1358–1364.
Higgins, J.A., Cooper, M., Schroeder-Tucker, L., Black, S., Miller, D., Karns, J.S., Manthey, E., Breeze, R., Perdue, M.L., 2003. Appl. Environ. Microbiol. 69, 593–599.
Hurtle, W., Bode, E., Kulesh, D.A., Kaplan, R.S., Garrison, J., Bridge, House, M., Frye, S., Loveless, B., Norwood, D., 2004. J. Clin. Microbiol. 42, 179–185.
Jayasena, S.D., 1999. Clin. Chem. 45, 1628–1650.
Labib, M., Zamay, A.S., Kolovskaya, O.S., Reshetneva, I.T., Zamay, G.S., Kibbee, R.J., Sattar, S.A., Zamay, T.N., Berezovski, M.V., 2012. Anal. Chem. 84, 8966–8969.
Mairal, T., Özalp, V.C., Sánchez, P.L., Mir, M., Katakis, I., O'Sullivan, C.K., 2008. Anal. Bioanal. Chem. 390, 989–1007.
Makino, S.I., Cheun, H.I., Watarai, M., Uchida, I., Takeshi, K., 2001. Lett. Appl. Microbiol. 33, 237–240.
Mock, M., Fouet, A., 2001. Annu. Rev. Microbiol. 55, 647–671.
Pagliarini, V., Neagu, D., Scognamiglio, V., Pascale, S., Scordo, G., Volpe, G., Delibato, E., Pucci, E., Notargiacomo, A., Pea, M., Moscone, D., Arduini, F., 2018. Electrocatalysis. https://doi.org/10.1007/s12678-018-0491-1.
Plotkin, S., Grabenstein, J.D., 2008. J. Infect. Dis. 46, 129–136.
Porchetta, A., Vallée-Bélisle, A., Plaxco, K.W., Ricci, F., 2012. J. Am. Chem. Soc. 134, 20601–20604.
Qi, Y., Patra, G., Liang, X., Williams, L.E., Rose, S., Redkar, R.J., DelVecchio, V.G., 2001. Appl. Environ. Microbiol. 67, 3720–3727.
Record Jr, M.T., 1975. Biopolym.: Orig. Res. Biomol. 14, 2137–2158.
Ricci, F., Plaxco, K.W., 2008. Microchim. Acta 163, 149–155.
Sheikhzadeh, E., CHamsaz, M., Turner, A.P.F., Jager, E.W.H., Beni, V., 2016. Biosens. Bioelectron. 80, 194–200.
Song, S., Wang, L., Li, J., Fan, C., Zhao, J., 2008. Trends Anal. Chem. 27, 108–117.
Swiecki, M.K., Lisanby, M.W., Shu, F., Turnbough Jr, C.L., Kearney, J.F., 2006. J. Immunol. 176, 6076–6084.
Tamborrini, M., Holzer, M., Seeberger, P.H., Schürch, N., Pluschke, G., 2010. Clin. Vaccin. Immunol. 17, 1446–1451.
Thavaselvam, D., Vijayaraghavan, R., 2010. J. Pharm. Bioall. Sci. 2, 179.
Tuerk, C., Gold, L., 1990. Science 249, 505–510.
Turnbull, P.C.B., 1999. J. Appl. Microbiol 87, 237–240.
Xiao, Y., Lai, R.Y., Plaxco, K.W., 2007. Nat. Protoc. 2, 2875–2880.
Yang, C., Wang, Y., Marty, J.L., Yang, X., 2011. Biosens. Bioelectron. 26, 2724–2727.
Zhou, L., Li, D.J., Gai, L., Wang, J.P., Li, Y.B., 2012. Sens. Actuat. B 162, 201–208.